XI PROCESSES OF "SPUNBOND"

The textile operations of spinning yarn and weaving are relatively time consuming – *ergo* – they are expensive. This was a good reason to search for a better solution, for a way to make flat textile products faster and thus less expensive. Two basic ways of accomplishing the goal are: glueing or welding the fibers together, or entangling the fibers in a permanent way while avoiding yarn twisting and weaving or knitting operations. These materials bear a common name, *nonwovens,* to express their origin in a nontraditional manufacturing process. Papers, where short cellulose fibers are held together primarily by polar forces, and felts made of wool where the fibers are enchained and hooked together by the natural scales on the fiber surface are the oldest nonwoven materials. The second half of the nineteenth century witnessed the development of felts from fibers other than wool by the way of entangling the individual fibers through a *needling* operation. The twentieth century came up with the invention of the name *nonwoven* for such materials, and with newer processes to make them.

The ultimate step, thus far, in reducing the costs of production of the textile flat structures was the development of the *spunbond* process. Some of the commercial processes produce material up to five meters wide at linear velocities exceeding five hundred meters per minute. The fiber formation and bonding are in one uninterrupted line which runs with velocities up to five hundred meters per minute, or even higher. The majority of spunbond processes, as taken by volume, uses fiber formation from the melt and fibers are bonded by thermal methods, utilizing thermoplastic properties of the polymers involved. The more important of the spunbond processes are described in the following pages since they involve fiber formation. Depending on the bonding methods, there are some requirements and/or limitations on the fiber properties, so these are discussed also.

From the point of view of mechanics, twisted yarn is a unique structure, The individual filaments have a helical conformation and are held together with the other filaments by frictional forces. Upon application of strain the helices become tighter, the normal forces acting on the individual fibers grow with increasing strain, the frictional forces increase appropriately. Without strain the yarn is soft and pliable, under strain it becomes tougher and stronger.[1,2]

Irrespective of the method of bonding the fibers together, the nonwoven web morphology resembles a rigid lattice, such as on a miniature iron bridge or high voltage power line. In consequence, the nonwovens are by nature stiff and papery; their morphology is somewhat similar to that of a paper. There are various ways to diminish some of the often unwanted properties, but it should not be expected that a nonwoven will duplicate the character of woven materials, as was the idea driving the developers of nonwovens. In effect, nonwovens are used primarily for inexpensive disposable products and for technical applications, and these applications have a bearing on the directions of the nonwoven development.

As it is difficult to put the different spunbond processes in any systematic framework, they are discussed here in accordance to the type of fiber formation,

whatever the bonding technique may be. The bonding techniques and their requirements are discussed in places of their relevance.

XI.1 Spunbond Formation from Melt

The first spunbond process was developed more or less simultaneously by Imperial Chemical Industries and by Du Pont De Nemours. The processes used essentially standard fiber formation from the melt, if there is such a thing as a standard process. In this case, we mean that the fibers are extruded, attenuated, and drawn by means of drawing rollers. Fibers are received from the drawing rollers by lay-down jets, which blow the fibers down on a moving belt which transports the fleece to the bonding section of the process.

Newer processes rely primarily on drawing jets. These are mostly *one step* processes, where the filament attenuation and the neck drawing are driven by one drawing jet, which serves at the same time as a lay-down jet. Drawing rollers are used when higher draw ratios are needed to obtain fibers with higher tenacities, but there are not many such demanding applications.

In some cases, a corona charge is put on the fibers just prior to the entry to the lay-down jets. The purpose of this is to prevent the fibers from clinging together, and at the same time to help them cling to the transporting wire belt, which must be grounded. The jets are operated with quite a large volume of air which is removed by suction applied under the transporter wire. Nonetheless, some portion of the air may bounce off the wire and adversely affect the uniformity of fiber deposition. The corona charge, or an electrostatic charge may prevent or reduce the effects of adverse air currents.

In spunbond formation from the melt, the fibers are bonded practically exclusively by utilizing their thermoplastic character. There are processes that rely on swelling of the fibers to make them tacky, but these processes are of lesser importance.[3] For thermal bonding, there are basically two systems of fiber formation with a number of subgroups or modifications.

Firstly, two different polymers with greatly different melting character may be used. Separate strands of fibers are formed from the two polymers, and the fibers blended before the deposition jets. This method offers many possible variations of hardware for blending and depositing the fibers. More frequently, however, side-by-side bicomponent fibers are made where one side (bonding side) of the fiber melts at a lower temperature, so the properties of the "matrix" part of the fiber deteriorate due to the heat exposure less than it would be the case for single component fibers.

Secondly, only one polymer may be used. Fibers are formed so that different melting characteristics are obtained. There may be separate strands with differing melting ranges. There may be segmented fibers, where the different segments melt differently.[4] The majority of spunbond processes, again judged by the production volume, are based on forming one strand of uniform fibers and bonding is performed by "welding" the fibers in discrete areas, by so called *point bonding.*

Whichever way the fibers are made, all the principles of fiber formation, as given in other chapters, must be obeyed. However, as is evident from the description given above, there are many different configurations a spunbond process may be given. Each of these configurations has more than one solution as the arrangement of the hardware is concerned. The bicomponent formation is usually a standard solution for such types of process, as described in section XII.3. Formation from two polymers in parallel means essentially two separate positions located side by side; the only difference is whether the threadline is lead through common rollers or if the whole machine must be duplicated.

In cases where one polymer is used with a differentiation of the melting characteristics, the number of possible solutions is much larger.[5,6] More often than not, the extrusion section is common both for matrix and binder filaments. In such cases a portion of fibers extruded from a spinnerette is diverted to a different formation for binder fibers. Another, more frequent design, feeds the polymer from a common extruder to separate spinning blocks for the binder formation. In the last named cases, one binder threadline usually cooperates with two neighboring threadlines of matrix fibers.

Segmented fibers are normally made in one threadline, one formation, and one drawing. The fibers entering the drawing zone pass through a take-up or feed roller which has hot and cold segments. Due to the difference in temperature, the draw ratio, as well as the thermal history, is different in the different segments. The obtainable difference in the onset of melting amounts to some two, to a maximum of seven degrees.

The processes which differentiate the matrix from binder fibers operate, as a rule, with positive (roller) transport. The majority of processes which do not differentiate the fibers operate with constant force (pneumatic jet) drawing systems.

If two polymers are used, then usually the binding fibers are made from the same polymer as the matrix fibers, but copolymerized with other monomers to change the melting characteristics. To change the melting characteristics of fibers made of the same polymer one must use the principle of melting temperature dependence on the crystallization temperature. Development of the appropriate conditions for the formation sector is rather involved. Drawing of the binder fiber must be performed also at a low temperature, and preferably to a lower draw ratio.

At this point it may be said that if the formation and drawing of the binder and matrix fibers are separate, there is a danger that the velocities for the two tows entering the lay-down jet will not be equal. Unequal velocities at this point of the process create frequent cobwebbing and jamming of the depositing jets, which causes expensive discontinuities of the process and is highly aggravating to the operators. When the two streams are separate for the whole path, inciuding the lay- down, obtaining proper distribution of the binder fibers may be difficult indeed.

Such are the often used possibilities with their good sides and pitfalls. Which of these ways may be more suitable for the conditions considered may be decided only in accordance with the choice of both the desired fabric properties and of the

boding method.

XI.1.a Meltblown

The original authorship of the meltblown process is difficult to establish with full certainty. It appears that first the process of meltblowing fine fibers for production of filter cartridges was developed by F. W. Manning[7] in 1946. Later, in 1954 a process for producing meltblown fibers was described by V. A. Wente of the U. S. Naval Research Laboratory.[8] Since that time, patents regarding meltblown are multiplying, but with little, if any, real innovation.

The principle of the process is given in figure XI.1. A polymer melt, preferably of low viscosity, is extruded from a capillary. On both sides of the capillary are located channels through which high velocity air is led as close, and as parallel to the extrudate as possible. The high velocity air simultaneously provides cooling and force to attenuate the filaments. There are many different variants for the design of such a meltblowing head. Low viscosity (low molecular mass) polymers are often used, despite the fact that this is counter productive from the point of view of fiber strength. However, the polymer pressure requirement is given special consideration in view of the unavoidable inherent mechanical weakness of the extrusion tip geometry. Some of the heads have capillary exits flush with the bottom line of the head, some put the capillary exit in a recess. Usually the capillaries are short, also because of the desire for low extrusion pressure.

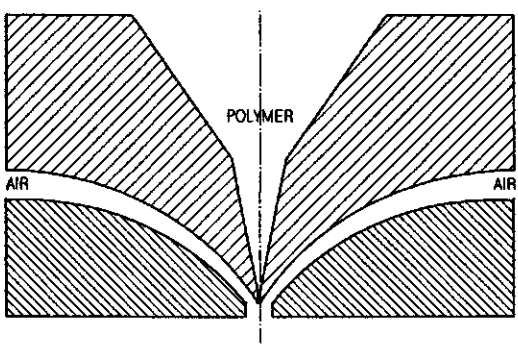

Figure XI.1: *Schematic drawing of a meltblowing head.*

From the theoretical point of view, the process must obey all the rules of fiber formation from the melt. One may say that this is a formation from the melt with pneumatic transport, where the air jet is to provide a pushing rather than a drawing force, while simultaneously providing for the quenching.

R. L. Shambough and co-workers have published attempts at a theoretical solution of the meltblown process at relatively low air velocities.[9–12] The efforts were concentrated on adopting the solutions published for fiber formation from the melt, in particular the works by Ziabicki, Petrie, Phan Thien, Kase and Matsuo. The experimental results agree with the theoretical calculations to a somewhat lesser degree than the similar solutions for the "classic" process of fiber formation from

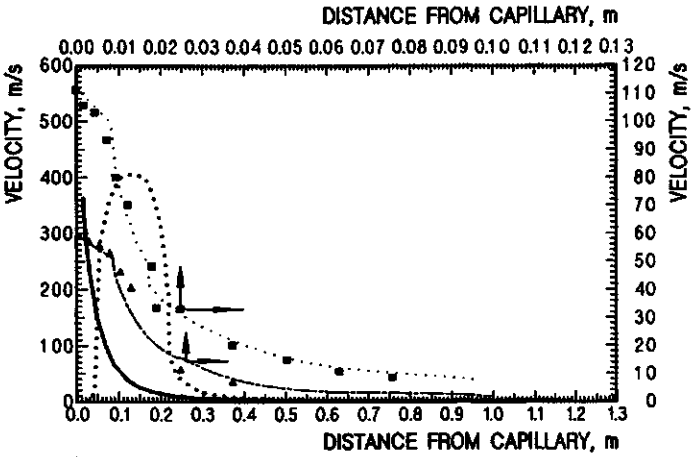

Figure XI.2: *Air velocity versus distance in meltblown processes: dashed and dot-dashed lines – low air velocity data after Uyttendaele and Shambough,*[12] *full drawn line air velocity close to sonic, heavy dotted line fiber velocity after H. Bodaghi.*[13]

the melt. In particular, the discrepancy between the calculated and experimental fiber diameter appears to be different by a factor of up to fifty.

Some portion of the problems preventing closer agreement between the theory and experiment may well constitute the treatment of rheology. A much larger problem, however, seems to be the treatment of aerodynamics. If to judge from the published sketches, the air flow up to the exit from the slot next to the exit of the capillary is not necessarily an accelerated one. This does not provide a guarantee of vortex free flow. The high velocity air discharged from the orifices looses its velocity very rapidly, as indicated by Shambough[10,11] and Bodaghi,[13] and shown in figure XI.2. Moreover, at some 40 *mm* to 50 *mm* from the exit of the capillary, the filament velocity exceeds the velocity of the drawing air, which indicates that the first impetus of air provides an appreciable momentum to the fiber to slow it down later.

One of the most common characteristics of aerodynamics is that vortices are practically always formed in a decelerating flow (see also section VI.1). As a consequence, the fibers start loosing momentum. Fast photography shows that the fibers form loops, which represents direct evidence of the air vorticity and allows us to infer that the fiber velocity is higher than air velocity. The last inferences have been confirmed experimentally by Bodaghi, [13] as shown in figure XI.2.

In summary, one may state that fiber formation in the meltblown process must obey the general principles ruling fiber formation from a melt, however, first the aerodynamics of the process need thorough scrutiny and definition. To apply the general principles of fiber formation from melt, some modifications must be introduced in respect to the decelerating forces of air drag over a large segment of the threadline.

There have been attempts to enclose the meltblown formation from the blowing head down. So far, such solutions have shown to be impractical, however. If the enclosure is close to the fibers, then major operational problems with the fibers sticking to the enclosing walls appear. If the enclosure is more spacious, then maintaining the air velocity requires so large a volume of high pressure air that the process begins to have problems with economy, not to speak of the removal of large volumes of spent air. Nevertheless, there seems to be a large room for inventiveness here.

The high acceleration of the extrudate immediately after leaving the capillary leads to the formation of very fine fibers; in commercial products the fibers range generally from $1\mu m$ to $10\mu m$, though submicron fibers are also obtainable. Additionally, rather small capillary diameters are in use. The decrease of the forces acting on the fibers and the deceleration of fibers exclude any possibility of cold drawing. This, naturally, leads to very low tensile strength of the obtained fibers. At the moment, the only potential improvement of this aspect of the product would be bidirectional drawing of a bonded fabric. Nonetheless, so far the applications of meltblown fibers have not required higher tenacities. The fibers are used primarily for application as filters of one sort or another, and there the materials work mostly in a compression mode, that is, transverse to the fiber axis. Where a higher strength is needed, the meltblown fibers are laminated with stronger spunbonded materials, which represents an entirely natural marriage.

Commercial meltblown products often have a wide distribution of fiber diameters, or outright, small clumps of polymer. Generally, this originates from the very low quality of polymers used for meltblowing. The most frequently used polymer – polypropylene – often is highly degraded with the help of peroxides to achieve low viscosity. However, the peroxides produce a lot of cross linking, gel. On the other hand, good quality polymer, free from cross linked (gel like) material, permits us to obtain very fine products with narrow distributions of fiber diameters, but there is a matter of price. Thermoplastic elastomers of a different nature are also used for meltblowing; some of them, those with very high molecular mass, may be diluted with parafine or similar materials. This is proof enough that slightly higher melt viscosity is not the problem reducing the quality of the meltblown fabrics.

The meltblown materials have some integrity of their own, without bonding, however, to improve their usefulness they are subjected almost exclusively to thermal bonding.

Despite its age, the meltblown process enjoys a modest commercial success. Additional developments, or perhaps modifications of the process, might boost the product applicability. Manufacturing of very fine diameter fibers is difficult and always expensive. Meltblowing has some potential in this respect.

XI.2 Thermal Bonding

Thermal bonding is executed with two different types of equipment: *through-air bonders* and calenders of several types. A schematic representation of the

principle of action of a through-air bonder is given in figure XI.3.[14] The fiber fleece is introduced between the surface of a large perforated drum and a wire belt which presses the fleece against the drum surface. Hot air is introduced into the chamber containing the drum and removed from the center of the drum. The direction of the hot air may well be reversed. In this way the hot air is forced to pass through the wire belt, through the fleece and drum perforation thereby providing the necessary energy to heat the fibers of the fleece. The pressure of the wire belt compacts the fleece and forces the fibers to more numerous and more intimate contacts.

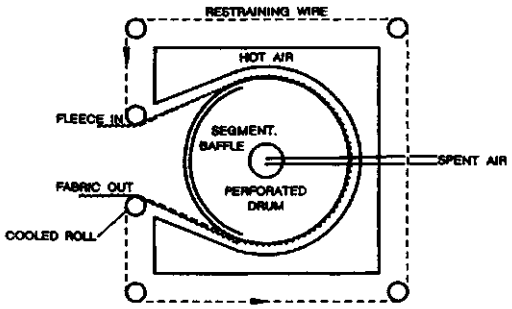

Figure XI.3: *Schematic description of the action principles of the through-air bonding. After T. A. Zack et al.*[12]

Zack and co-workers[14] devised a way to calculate heat transfer in a through-air bonder. The equations are not quoted here since they seem to contain more simplifications than necessary.

Generally, through-air bonding is well suitable for thick materials. Since the number of fiber-to-fiber contacts is large, this method of bonding gives better results with matrix and binder fibers, otherwise the number of bond points may be too large, leading to a stiff fabric. By the nature of the method, compacting of the fleece is moderate, so the resulting fabrics have a tendency to be thick, low density.

The most frequently used method of bonding appears to be by the way of calenders. The rollers used may have plain surfaces or may have pins arranged in some pattern. In the past, rollers with rubber surfaces were also used to increase the area of the nip, that is, to increase the residence time of the fabric in the roller nip.

It has been shown that heat transfer directly from a metal surface to the fibers is very small, thanks to limited contact due to the curvature of fiber surface and due to the generally unfavorable heat transfer coefficients on metal-polymer interfaces.[15] Much more efficient is the heat transfer *via* convection with air as the carrier.[14,15] S. B. Warner[16] stressed the importance of the adiabatic heat generation due to compression.

Considering the heat transfer possibilities, one may conclude that the through-air system is a good one, if the relatively low compaction pressure and not very high maximally obtainable speed are acceptable from the other standpoints. The most

favorable thermal bonding system is discrete point bonding with calender rollers equipped with bonding pins. Since essentially the entire load in the calender nip is concentrated on the bonding pins, pressure there is very high and such is the adiabatic heat generation. The material which finds itself between the pins is exposed to much lower temperature and pressure, thus the majority of the fibers suffer much less damage. The degree of bonding may be regulated by the size, distribution and the total area of the bonding pins in relation to the entire surface, a separate binding fiber is not needed.

A comprehensive analysis of the heat transfer to a fleece in a calender nip has been done, considering all aspects of the process. No shortcuts were taken *a priori*, relatively few simplifications were used, the results of the calculations were used to decide the significance of different aspects of the process.[17] The results are applicable to calenders with plain rolls, to point bonding, and to spiral rollers.

For these considerations, the calender nip was defined as the angle (or the corresponding length of the roller circumference) between the center point of the contact of the two rollers and the point where the rollers' separation is equal to the thickness of the uncompressed fleece. This means that at the moment the compaction of the fleece begins, the fleece enters the nip. From this assumption it results that the size of the nip increases with the increasing "fluffiness" of the heated material and with its surface weight. More justifications for such a definition will become apparent as the consideration progresses. A schematic picture of a nip is given in figure XI.4.

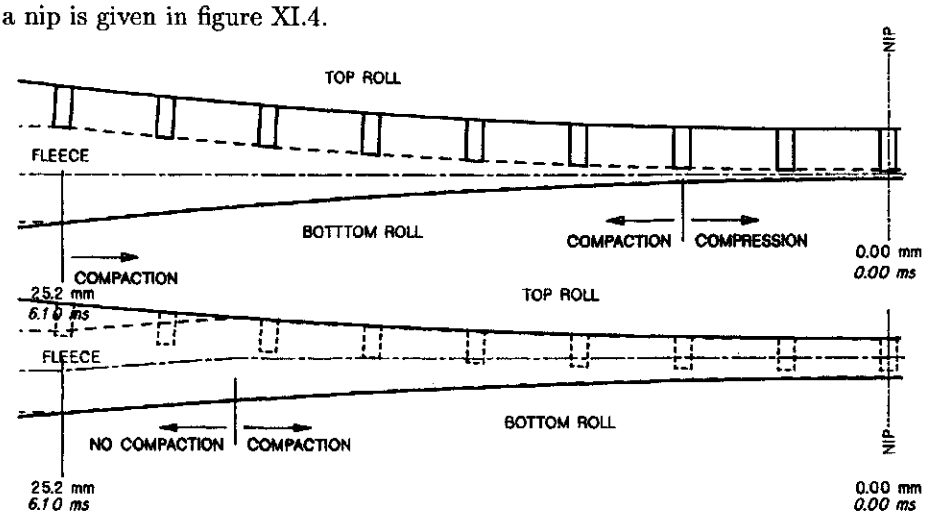

Figure XI.4: *Schematic depiction of the calender nip: top – for bonding pins, bottom – areas between the pins. After Z. K. Walczak.*[17]

For rollers with a pattern, the first point of contact is the contact with the pins. Of course, the areas between the pins enjoy more freedom of space. For the case of point bonded materials, the gap between the rollers is determined to be the thickness of a solid film of the fiber polymer minus a certain amount of material which is squeezed out of the bond point area. The squeezed amount depends on

the temperature and pressure of the operation and on the polymer viscosity at the existing conditions.

The calculation of heat transfer consists here of two segments. One segment treats the fibers individually before compression, and with respect to their location in the nip (the distance from the top and bottom rollers); these calculations may be done according to those for quenching fibers (see section VI.2). The second segment considers the individual fibers being compressed in groups of various numbers of fibers, and of fibers originating from the different locations in the cross section of the fleece. In this way, the results depict the inhomogeneities in the bond point formation. The second segment of the calculations considers only the "vertical" heat transfer. In the "horizontal" direction there is both mass and heat transfer, which so far has not been defined. Full description of this process would require a very large number of assumptions, many difficult to verify. Considering this and the unavoidable inhomogeneities existing during the bond formation, more detailed calculations may not be worth the effort needed.

For the first segment the heat balance is as follows.

$$q_r - q_d = q_c \tag{XI.1}$$

where

$$q_d = v\ da\ T_d\ \rho\ C_p \tag{XI.2}$$

$$q_r = v\ da\ T_r\ \rho\ C_p \tag{XI.3}$$

Here q is heat flow, v is fiber velocity, a is cross sectional area of the fiber, T is temperature, ρ is polymer density, C_p is the specific heat of the polymer of the fiber. The subscripts d and r mean delivered and removed, respectively.

The conductive heat transfer is according to the Fourier's equation:

$$q_c = -\lambda_p\ \nabla^2\ T\ da\ dl \tag{XI.4}$$

Here λ_p stands for heat conductivity of the polymer of the fiber, ∇ is the Laplacian, and l is the length of fiber along its axis.

After substitution of equations XI.2 and XI.3 into XI.1, and after substituting $v = dl/dt$ (where t is time) we have

$$\frac{dl\ da}{dt} dT = \frac{\lambda_p}{C_p\ \rho} \nabla^2\ T\ dl\ da \tag{XI.5}$$

and in a developed form it becomes

$$\frac{dT}{dt} = \frac{\lambda_p}{C_p\ \rho} \left(\frac{\partial^2 T}{\partial r^2} + \frac{1}{r} \cdot \frac{\partial T}{\partial r} + \frac{\partial^2 T}{\partial l^2} \right) \tag{XI.5 a}$$

where r is the radial distance from the fiber axis. Time may be eliminated from equation XI.5a by taking advantage of the equation for fiber velocity.

$$v = \frac{dl}{dt} = \frac{V_f}{\pi R^2} \tag{XI.6}$$

Here V_f stands for the volume of a single fiber of d_t weight titer moving through the calender per second. In the case of d_t in denier this leads to

$$V_f = d_t \cdot \frac{v}{900000\ \rho\ \pi\ R^2} \tag{XI.7}$$

In view of the above, and introducing normalized variables, θ for temperature and u for radius equation XI.5 obtains the form:

$$Z \cdot \frac{\partial \theta}{\partial l} = \frac{1}{u} \cdot \frac{\partial}{\partial u} \cdot u \frac{\partial \Theta}{\partial u} + R^2 \cdot \frac{\partial^2 \theta}{\partial l^2} \tag{XI.8}$$

where

$$Z = \frac{d_t\ v\ C_p}{900000\ \pi\ \lambda_p} \tag{XI.8 a}$$

The second term in the right hand side of equation XI.8 is dropped as very small. The boundary conditions are set as $T = T_a$ for all $l = 0$ and T_a is the ambient temperature. Next one may define

$$dq = \alpha\ T\ ds \tag{XI.9}$$

where α is heat transfer coefficient, $ds = 2\pi\ R\ dl =$ *surface of a fiber segment.*

From Fourier's equation (equation XI.4) results

$$dq = \lambda_p \cdot \frac{\partial T}{R\ du}\ ds \Big|_{-u=1} \tag{XI.10}$$

Equations XI.9 and XI.10 determine the spatial boundary condition:

$$\frac{\alpha R}{\lambda_p} = \frac{1}{T} \cdot \frac{\partial T}{\partial u} \Big|_{u=1} \tag{XI.11}$$

The dependence of heat conductivity on temperature for polypropylene, the polymer most frequently used for spunbonded fabrics, one may determine from the Weber formula[18]

$$\lambda_p = \lambda_p^0\ C_p\ M_w^{0.333} \rho_p^{1.333} \tag{XI.12}$$

where M_w is weight average molecular mass, λ_p^0 is heat conductivity at $0°C$. The last value for polypropylene[19] is $3.0871 \cdot 10^{-5}$. Heat capacity for polypropylene may be calculated from the weighed average of heat capacities calculated for solid (about 50 % crystalline) and noncrystalline fractions. For the solid: $C_p = 0.00136T°C + 0.4120\ cal/g$ For the molten: $C_p = 0.001223T°C + 0.3809\ cal/g$.

The left hand side of equation XI.11 may be written using Nusselt number ($Nu = \alpha\ D/\lambda_a$)

$$\frac{\alpha\ R}{\lambda_p} = \frac{Nu\ \lambda_a\ \Delta T}{2\ \lambda_p} \tag{XI.13}$$

In addition to the heat transferred through the air, heat is also transfered *via* radiation. This may be calculated using Stefan-Boltzmann law

$$E_r = \epsilon\ \sigma\ T^4 \tag{XI.14}$$

where E_r stands for radiation energy, σ is the Stefan- Boltzmann constant [$\sigma = 5.7686 \cdot 10^{-8} j/(m^2\ s^\circ K^4)$], and ϵ represents the material emissivity. For polypropylene, the emissivity has been determined to be $\epsilon = 0.92$ to 0.93, while for oxidized metal surfaces (roll surface) it is $\epsilon = 0.7$.

The rate of heat exchange between two surfaces of areas F_1 and F_2, with temperature T_1 and T_2, respectively, is

$$\dot{q} = \sigma(T_1^4 - T_2^4)F_1\ \psi_{12} = \sigma(T_1^4 - T_2^4)F_2\ \psi_{21} \tag{XI.15}$$

Here ψ is shape-emission coefficient equal

$$\psi_{12} = \left[\frac{1}{\psi_\rho} + \left(\frac{1}{\epsilon_1} - 1\right) + \frac{F_1}{F_2} \cdot \left(\frac{1}{\epsilon_2} - 1\right)\right]^{-1} \tag{XI.16}$$

Here ψ_ρ represents the shape-refractive coefficient which for the case of a fiber and a relatively large plane may be assumed to be around 0.9,, as for very long rectangles. In spunbonded materials, the fibers are usually at an angle, ranging from 30° to 45°, to the surfaces. For this reason, the value of ψ_ρ amounts to between 0.67 and 0.83 (1 is for 90°). In the considered case, one half of the fiber faces one roll surface, the other half faces the other roll surface.

Equations XI.15 and XI.16 may give a more convenient formulation of the heat transfer coefficient in radiation.

$$\alpha_r = \sigma\ \psi_{12}\left(T_1^4 - T_2^4\right) \tag{XI.17}$$

In consequence of the consideration of heat transfer through radiation, another term representing radiation must be added to equation XI.13

$$\frac{\alpha\ R}{\lambda_p} = \frac{Nu\ \lambda_a\ \Delta T}{2\ \lambda_p} + \frac{(\lambda_{r1} + \lambda_{r2})\ R}{2\ \lambda_p} \tag{XI.18}$$

The heat transfer coefficient, λ_r, ought to be calculated for both the top roll and bottom roll temperature differences in case they are not equal.

The contribution of radiation to the overall heat transfer is not very large, but it is by no means negligible. Practical calculations show that the radiation contribution results in some three to ten degrees temperature increase, depending on the other conditions. In terms of crystal melting, such a temperature difference may be equivalent to the additional melting of ten to even twenty per cent of crystals.

Obtaining of the heat transfer coefficient between the fibers and the surrounding air requires additional considerations. When fleece moves gradually into the calender nip, the available volume decreases. The volume of fibers remains constant, naturally, and the air entrained between the fibers is gradually expelled. In aerodynamics, any formal studies of such a case are not available. To cope with the problem, the following speculation is offered with the help of figure XI.5.

If one considers the fleece element with volume V_5 moving forward to replace the element V_4, the volume of air flowing through the cross section of the elements

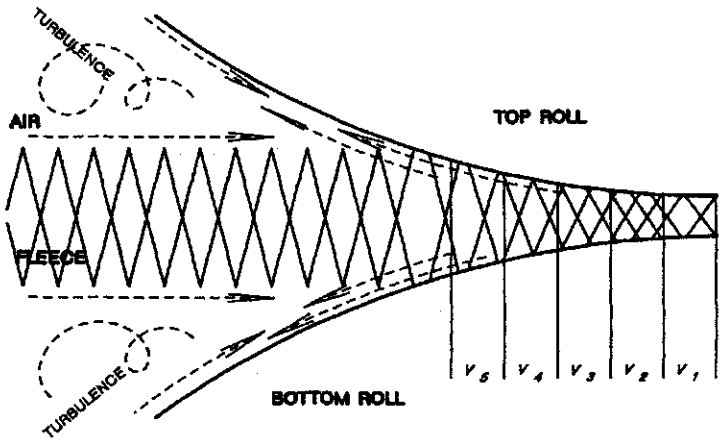

Figure XI.5: *Schematic depiction of the air flow in the nip of a calender. The dashed lines depict the expected paths of air. After Z. K. Walczak*[17]

5 equals V_5. Such a decrease of the volume continues all the way to the minimum of the nip cross section. At the minimum there is either practically no air left, like in the bond points, or there is some minimum volume in the areas outside of the bond points. In this way, there is a constant stream of air "backing up" toward the entry to the nip. One may well expect that the warmer air from elements V_1, V_2 mixes with the colder air of the earlier elements V_5, V_6, moving in with the fresh portions of the cold fleece.

The multitude of fibers inside of the fleece represents strong resistance to the air flow. The squeezed air must then seek a path with a lower flow resistance, and this will be closer to the roll surface, particularly in the area of the first contact between the roll and the fleece. As a result, one may assume that there is a gradient of air flow, the lowest velocity being in the center of the fleece and the highest at the roller surface. Such an gradient of air flow will lead to a temperature gradient across the fiber assembly, from its surface to the center.

It is doubtful whether such a situation exists over the entire extent of the nip, however, it may be in the areas between the bond points. In the areas of bonding pins ultimately there is no air left, so in the final segments there is probably a much smaller air velocity.

The roll surfaces outside of the nip area are in contact with air of approximately ambient temperature. The rolls must certainly have some pumping action, and so does the moving fleece. The "fuzzy" surface of the fleece may cause its pumping action to be even stronger than that of the rolls. In consequence, there are two air streams heading toward the nip and colliding at the entry. It would be difficult to admit that the colliding air displaces the air entrained in the fleece. While the air brought by the fleece has ambient temperature, the air pumped in by the roll must be substantially warmer.

The aerodynamic situation in the nip, as ill defined as it is, does not allow

us to calculate the temperature distribution accurately. As a consequence, the heat transfer in the calender nip cannot be calculated with full accuracy, certain approximations are needed.

The approach adapted here was:

1. Neglecting the "back flow" of air, the air temperature distribution was calculated using conventional engineering methods.
2. Using the obtained temperature distribution, numerical methods were used to perform a "mixing" operation. The hotter air flowing back has been given a parabolic velocity distribution across the nip thickness.
3. The mixing procedure has been iterated several times, but the results stopped "being reasonable" after the third iteration. To remain on the safer side, only two iterations have been accepted.
4. The resulting air temperature distribution has been described in general terms in a simplified way.

The (maximum) air temperature near the top roll for the $i-th$ volume (or cross section element) is

$$T_{mt} = T_{rt} - 2T_{amb}\frac{N_i - i}{n_i} \tag{XI.19}$$

For the bottom half of the fleece, it is

$$T_{mb} = T_{rb} - 2T_{amb}\frac{N_i - i}{n_i} \tag{XI.20}$$

Here T_{mt} and T_{mb} is maximum air temperature near top and bottom roll, respectively; T_{rt} and T_{rb} is roll temperature top and bottom, respectively; N_i is the total number of elements considered in the calculation, and i is the sequential number of the element. At the point of roll-to-roll contact $i = N_i$ (contrary to figure XI.5).

The distribution of temperature across the fleece, the thickness of which is defined as the number of single fiber layers in the fleece, N_y, for the case when the upper roll is the hottest, is for the upper half:

$$T(i,j) = T_{mt} \cdot \left[\frac{(j - 0.5\ N_y)}{(0.5 \cdot N_y)}\right]^p \tag{XI.21}$$

and for the bottom half:

$$T(i,j) = T_{mb} \cdot \left[\frac{(0.5\ N_y + 1 - j)}{(0.5 \cdot N_y)}\right]^p \tag{XI.22}$$

When the top and bottom roller temperatures are the same, or when the bottom roll temperature is lower, the equation may be written as follows.

$$T(i,j) = T_{mt} \cdot \left[\frac{1}{(0.5 \cdot N_y)}\right]^p + T_{mb} \cdot \left[\frac{(0.5 \cdot N_y + 1 - j)}{(0.5 \cdot N_y)}\right]^p \tag{XI.23}$$

where j is the consecutive number of the fiber layer, counted from the bottom of the fleece; and $p = 2L_i$, when L_i is the gap between the rolls for the considered element.

Using a so assumed air temperature distribution one may calculate the Nusselt number as given in section VI.2.a. At this point, all the needed input data are secured and one may solve equation XI.8 for the different locations in the fleece. The method of solution is essentially the same as in section VI.2.a.

When a fiber reaches a temperature in the melting range, then the heat effect may by no means be taken as negligible. Using the actual integral melting curve, it is necessary to determine the slope of crystal melting *versus* temperature, $d\alpha/dT$, for a given segment of the fiber cross section. Based on the melting crystals, one may calculate the heat effect, or rather, the temperature decrease caused by the heat loss due to melting.

$$T_d = \frac{d\alpha \; \alpha \; H_m \; \Delta T_r}{dT \; w \; \Delta x \; C_p} = \Upsilon \; \Delta T_r \tag{XI.24}$$

Here w is the fiber weight titer adjusted to the used system, Δx is the length of the fiber interval used in the calculations, C_p is specific heat of the polymer, α is degree of crystallinity, ΔT_r is the actual temperature increase from the previous segment, H_m is the heat of crystal melting. The last quantity is not exactly constant and ought to be calculated separately for crystals grown at different temperatures. The net effect of the fiber temperature change may be conveniently obtained from the following equation.

$$\Delta T_r = \Delta T_i - T_d = \frac{\Delta T_i}{(1 + \Upsilon)} \tag{XI.25}$$

Here ΔT_i is increase of the temperature over the previous segment due to the heat transfer.

All of the temperatures are taken as relative values, usually divided by the maximum roll temperature.

Figures XI.6 and XI.7 present results of the calculations for two cases of bonding: at approximately correct temperature, and with somewhat excessive heat, respectively. At the top of each of the figures are calculations of temperature between the bonding pins and at the bottom of the graphs what happens under the bonding pins is shown. In the latter case, the final bond compression stage is shown separately; temperatures are given across the fiber radius for the surface and for the center of the fabric. For the more correctly heated material, the fibers between the pins never reach the temperature where the melting of crystals begins; this threshold is crossed only in the bond sites. In the second example, figure XI.7, the surface layer of the fibers between bonds do reach initial melting point. In the data presented in both of the figures, heating due to the impact compression has not been included.

The calculations of heat generation due to impact compression require some additional comments. The fiber distribution in a fleece, irrespective of the opinions based on macroscopic estimates, are never ideal in a microscopic sense. In view of

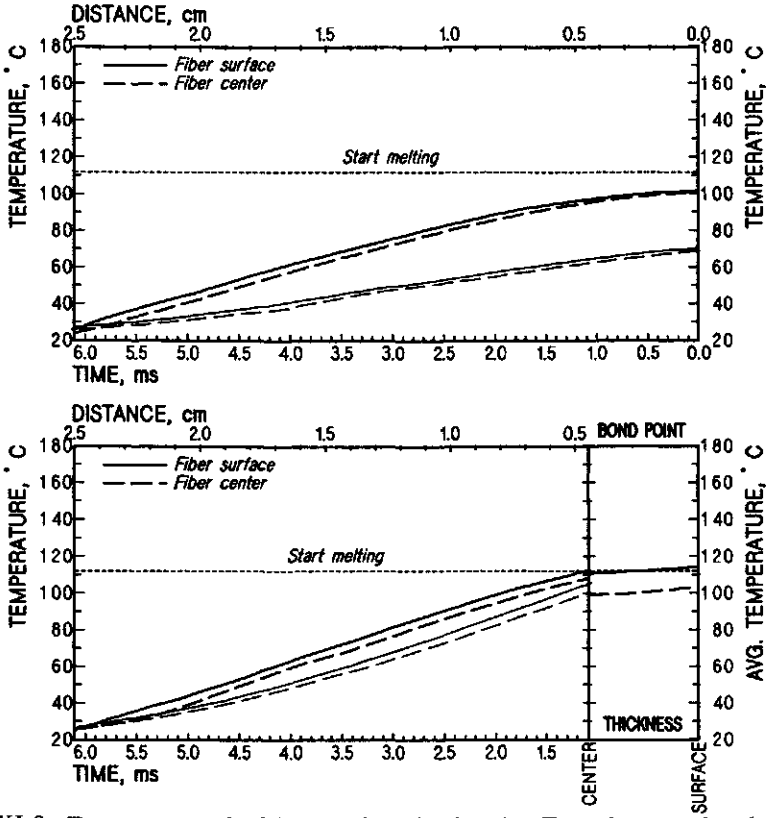

Figure XI.6: *Temperature of a fabric in the calender nip. Top – between bonds, bottom – under bonding pins. Correct heating, low pressure. Heavy lines - - surface of the fleece, fine lines – center of the fleece. No impact heat included.*

the small dimensions of the bond points, and even much smaller dimensions of the fiber diameter, the fiber distribution is never even and this in consequence leads to the formation of inhomogeneous bonds. A typical case, especially important for light weight fabrics, is presented by the photomicrograph of figure XI.8.

If the fibers are parallel to each other, there is a danger that under the pressure of a small bonding pin, room permitting, the fibers may spread into a monofiber layer. Fibers crossing each other have a smaller chance for such an escape. In addition, there is a question as to how many fibers may find themselves in one fiber cross section, their thickness, and from which location in the fleece cross section they originate. As it may be seen from figures XI.6 and XI.7, the fiber temperature is not uniform. As usual in similar situations, the uniformity of fiber distribution increases with the number of filaments, that is, with the surface weight of the fabric.

Calculations of the effect of impact compression lead to a number of possibilities. In figures XI.9 and XI.10 results of just such calculations are presented. Figure XI.9 – top corresponds to the heating conditions of figure XI.6, and the results given in figure XI.9 – bottom correspond to the case from figure XI.7. The

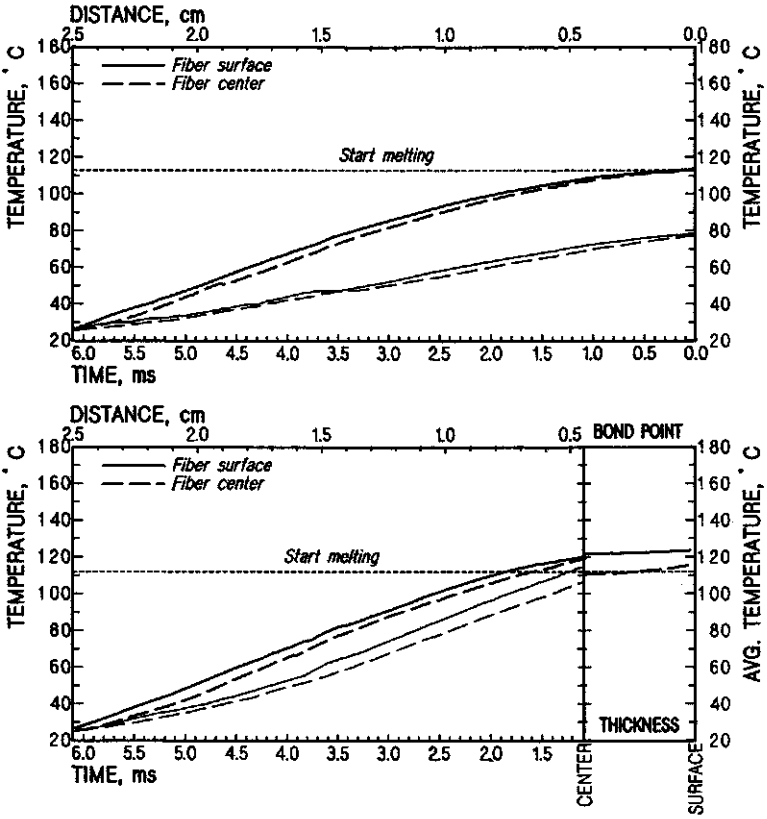

Figure XI.7: *Temperature of a fabric in the calender nip. Top – between bonds, bottom – under bonding pins. Too high heating, low pressure. Heavy lines – surface of the fleece, fine lines – center of the fleece. No impact heat included.*

same is true of figure XI.10 which shows the extent of the crystal melting *versus* bond thickness, where zero represents the bottom surface. Each of the figures presents the calculations of four different possibilities:

1. Four fibers *per* crossing, all from or near the top surface of the fleece – full drawn line.

2. Two fibers *per* crossing, both from the center of the fleece – dashed line.

3. Two fibers *per* crossing, both from the bottom surface of the fleece – dot - dash line.

4. Four fibers *per* crossing, two from the top and two from the bottom surfaces – dot - dot - dash line.

As the figures show, the different cases lead to markedly different results. As may be seen in figure XI.11, in real fabrics such situations really do exist. The figure presents photomicrographs of a 1 μm thick cross section of a bond point, cut perpendicularly to the fabric surface. The fabric is middle weight, too lightly

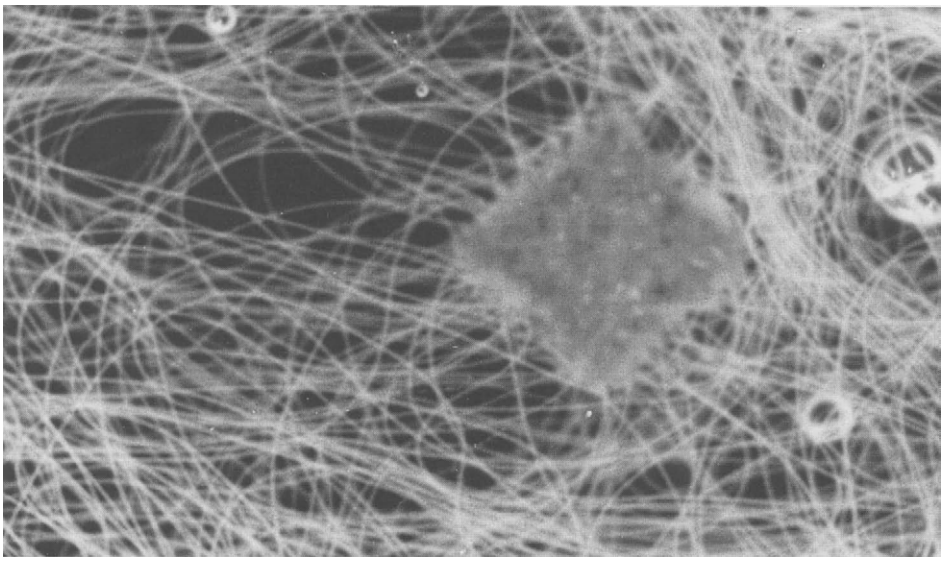

Figure XI.8: *Photomicrograph of a bond point in a lightweight fabric with not very uniform fiber distribution. Despite the high degree of fusion, nonuniformities of the bond point are visible.*

bonded, so the bond shows a tendency to disintegrate. One may see that the fibers adhere lightly, only a thin surface layer must have melted. The fiber cross sections, particularly those in the center of the fabric, are almost unaffected. Some fiber fusion did take place on the top surface of the fabric.

From the comparison of the figures, it is quite clearly evident how great a role the impact compression force plays in bonding. It is mostly a very positive role. As an optimum bonding situation one may define such a set of conditions which leads to the formation of strong bond points, while simultaneously the segments of fibers connecting the bond points are not permitted to lose their strength due to excessive heat exposure. The demands are high and perhaps difficult. To rephrase them, the fiber must be melted in a limited area of bond point and the rest of its length must stay as "cold" as possible. Reality does not permit full realization of this ideal, but closeness to the ideal condition may certainly be accepted as a determinant of the quality of the operation.

As difficult it may be to attain the ideal conditions in point bonding, it is still substantially easier than in any other operation of thermal bonding, as no other thermal bonding process known today offers the possibility of impact compression heating in discrete areas under largely controlled conditions. And this is the only thermal bonding operation known today which is able to provide well delineated, localized heating areas. To demonstrate the advantage more clearly, figure XI.12 shows also the temperature of a bond point of material with the more intense heating, as in figure XI.7, but the top graph shows a case with the generation of heat due to impact bonding omitted. This corresponds fairly closely to the

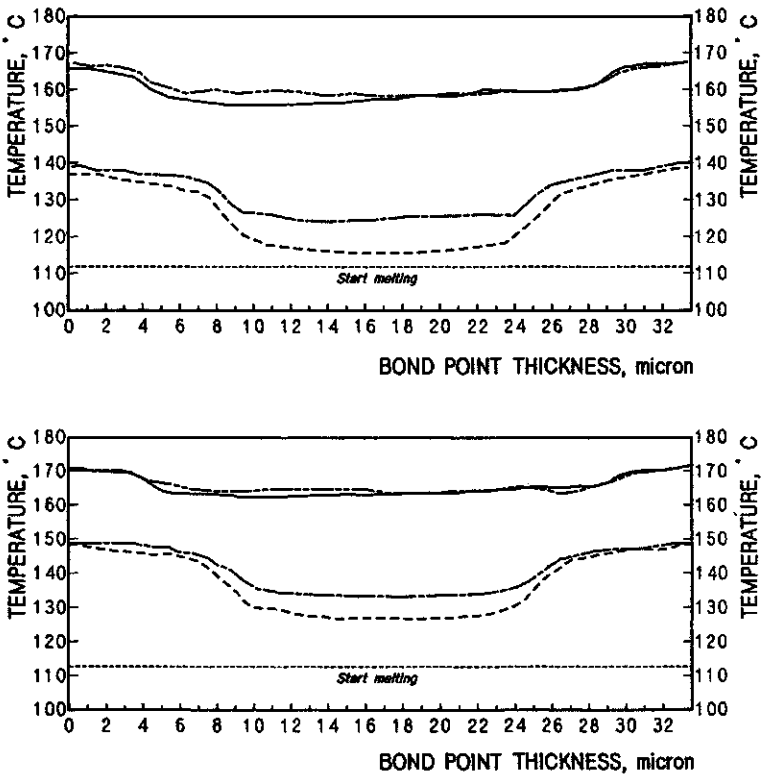

Figure XI.9: *Temperature of the cross sections of a bond point. Heat effect of the impact compression included. Top – heating from figure XI.6; bottom – heating from figure XI.7. Detailed explanation in text.*

condition obtainable in a plain roll calender or even through-air bonder. The bottom graph of figure XI.12 shows the same conditions with application of a higher bonding pressure, that is, with stronger generation of adiabatic heat. Figure XI.13 gives the melting of crystals in a bond point produced under the conditions of figure XI.12 – bottom. The bonding is, no doubt, excessive.

Due to the different bonding pressure in figure XI.12 – bottom and in figure XI.13, there is a somewhat different "fiber mix" than in figures XI.9 and XI.10. Here the combinations are as follows:

1. Five fibers *per* crossing, all from or near the top surface of the fleece – full drawn line.

2. Three fibers *per* crossing, all from the center of the fleece - - dashed line.

3. Four fibers *per* crossing, all from the bottom surface of the fleece – dot - dash line.

4. Five fibers *per* crossing, three from the top and two from the bottom surfaces – dot

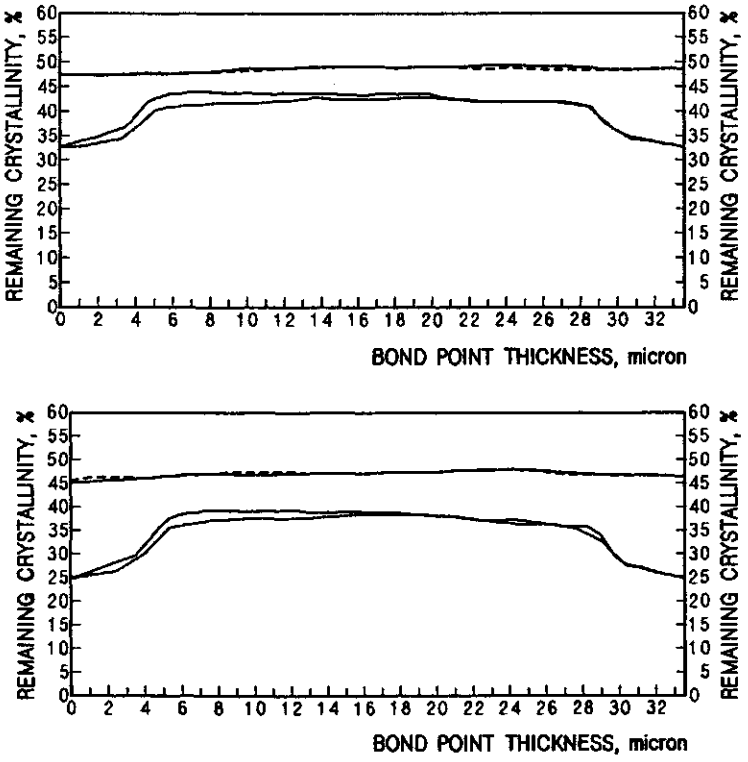

Figure XI.10: *Melting of the crystals in a bond point. The figure corresponds to figure XI.9. Detailed explanation in text.*

Figure XI.13 shows that the combinations 1 and 4 give the same result, fully superimposed lines, with crystallinity over a great majority of the bond point equal zero. Combination three gives results very close to those of combinations one and four. Only combination number two, all fibers from the center, has some 17 to 21 per cent of crystallinity left of the 50% determined for the fibers before bonding. The case without application of adiabatic heat generation, not shown in the figure, yields crystallinity of about 48 to 49% throughout the bond thickness; this means barely a surface softening.

Closer examination of the fiber cross sections in the bond sites shown in figures XI.8, XI.14, and XI.16 leads to the conclusion that the majority of fibers, even after being severely deformed, do not lose their identity totally. Even when the fibers are fused to form a block, the individual fibers, or their remnants, may be recognized; the optical properties of the oriented structures survive. Measurements of birefringence on bonded fiber cross sections indicate that the fibers, or better what were fibers, are still birefringent; the birefringence is highest along the fiber axis and decreases toward the surface.

The behavior of fibers in bonding, naturally, depends on the viscosity of the polymer melt under the bonding conditions. The portion of fibers which melts

completely and is heated to the point of relatively low viscosity is to a large extent

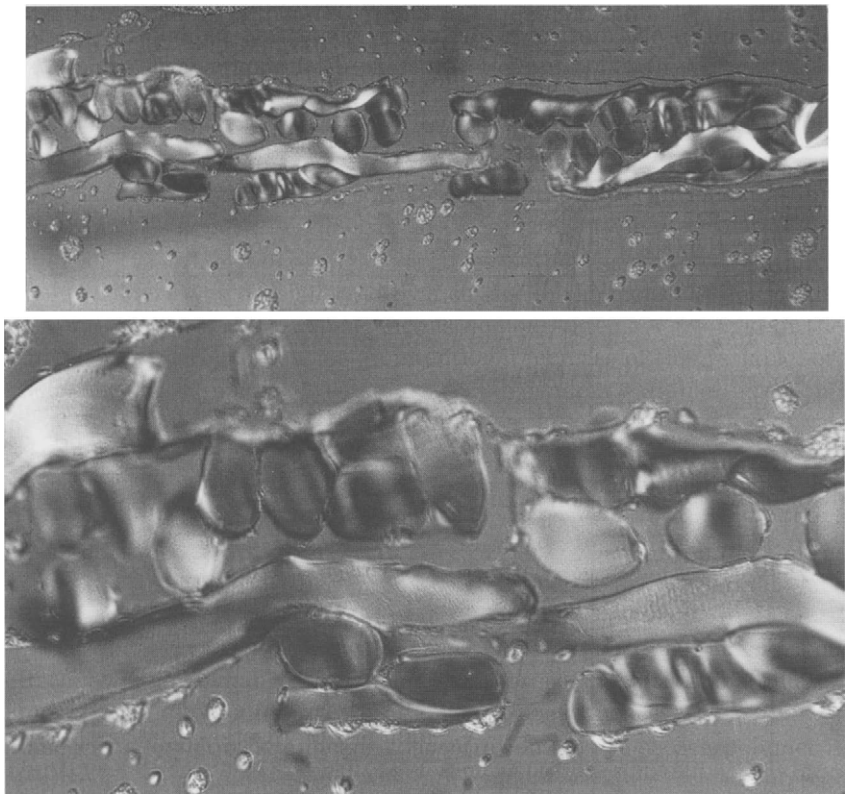

Figure XI.11: *Photomicrograph of a cross section of a bond point showing uneven, incomplete bonding and a tendency to disintegrate. Bottom – same at a higher magnification.*

expelled from the bond point to its perimeter. Some portion of the melt may fill the voids between the individual filaments, and all of it serves as a heat transfer agent delivering the heat to the unmelted fiber segments.

The calculations quoted above do not take into consideration the lateral heat flow, which for fibers and polymer melts is quite small and may be neglected. When the polymer if forced to flow, however, this represents a different story. There seem not to be enough justifiable assumptions to start contemplating the direction, intensity, extent of the flow and the connected heat transfer or conduction.

The effect of the point bonding process on overall crystallinity is presented in table XI.1, which presents experimental data on polypropylene fibers bonded in close to optimum conditions. Interpretation of the data given in the table XI.1 is not completely clear. An increase of the degree of crystallinity between the bond points may easily be ascribed to an annealing-like effect caused by the heat. The decrease of crystallinity in the bond points may be explained by a far reaching

melting and extremely short residence time in the nip. Past the nip exists a

Table XI.1
Crystalline properties in polypropylene fibers before and after point bonding.

Specimen	Crystal-linity %	Begin melting °C	Peak melting °C	End melting °C
Unbonded fiber	50.4	112	170	195
Bond points	42.3	119	167	192
Between bonds	54.5	138	166	187

Data from differential scanning calorimetry.

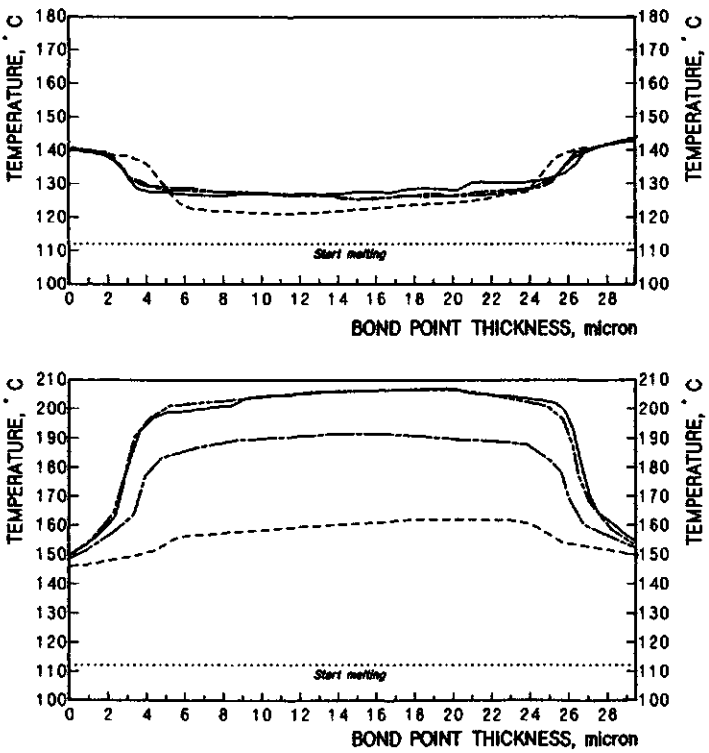

Figure XI.12: *Temperature distribution in a bond point. Case similar to that in figure XI.10. Here the top graph is without adiabatic heat generation, and the bottom shows a case with higher bonding pressure and somewhat different fiber combinations. Details in text.*

situation reverse to that before the nip; the fabric recovers to some extent from the compaction and admits air, but the air at this location is much cooler. In effect, at a lower temperature and without strain, the polymer may crystallize to a smaller extent. The shift in the temperature of the beginning of melting may

also be explained by an annealing effect. However, there is no good explanation

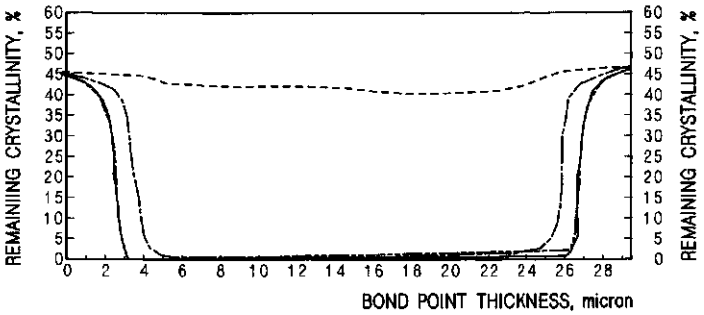

Figure XI.13: *Crystal melting in a bond point. Case from figure XI.12 – bottom, strongly overbonded. Details in text.*

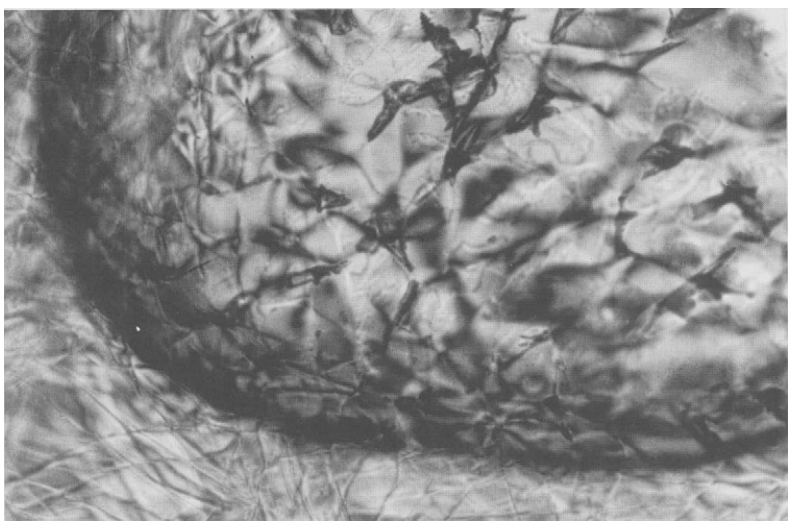

Figure XI.14: *Photomicrograph of an overbonded bond point, top view, showing some portion of the polymer expelled to the perimeter. Similar to the case given in figure XI.13.*

for the decrease of the peak and final melting temperatures. The $3°C$ to $4°C$ decrease is too large to be explained by the entropy changes, particularly since the fibers were drawn only to a modest degree. The only tentative explanation may be that these are the results of a recrystallization in the presence of some surviving crystal embryos; fibers retain their identity past the bonding process. However, why the highest melting elements were to suffer more remains unclear.

The methods of thermal bonding, other than point boning, may be treated in the same way as the heat transfer considered here. Naturally, for through-air

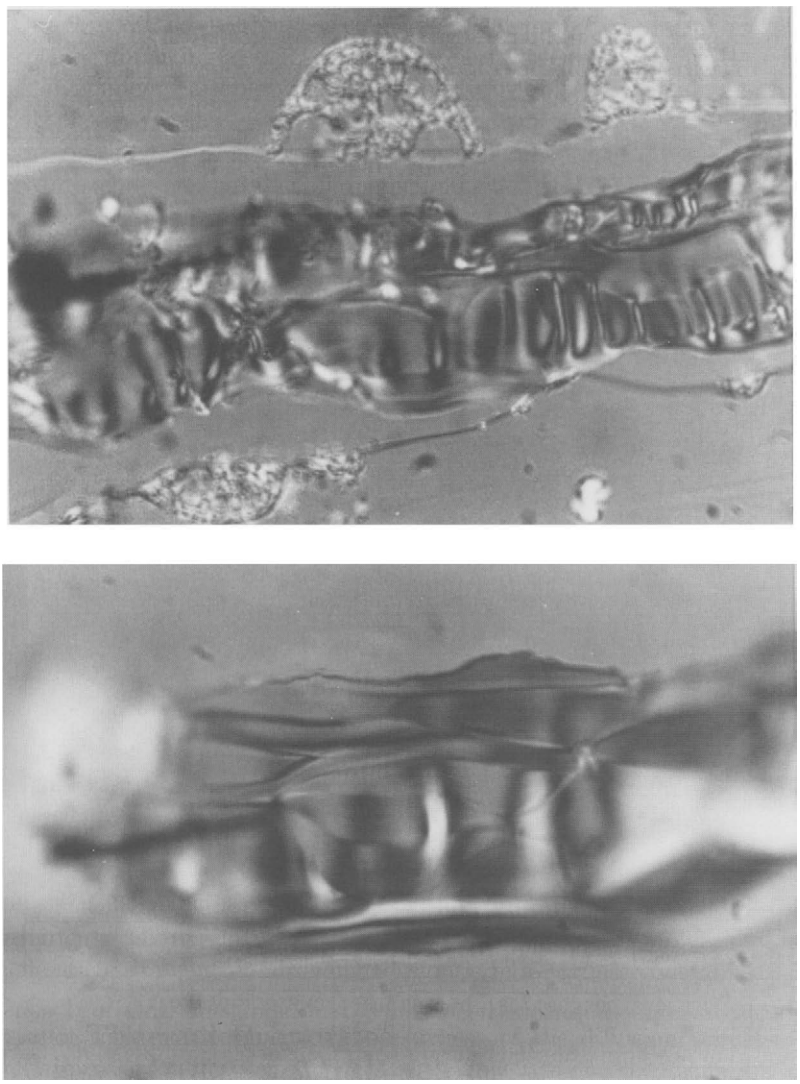

Figure XI.15: *Cross section of a bond point, similar to the overbonded case given in figure XI.13, medium weight fabric. Bottom, same specimen at higher magnification. Cross section 1μm, differential interference contrast.*

bonding it is necessary to omit the adiabatic heat generation due to the impact compression. In the case of plain roller calender bonding, there is some impact force to be considered on every fiber crossing which stands above the nip gap setting. It is usually many crossings and the load is distributed on all of those crossings, what results in a low adiabatic affect and a large number of bonds with

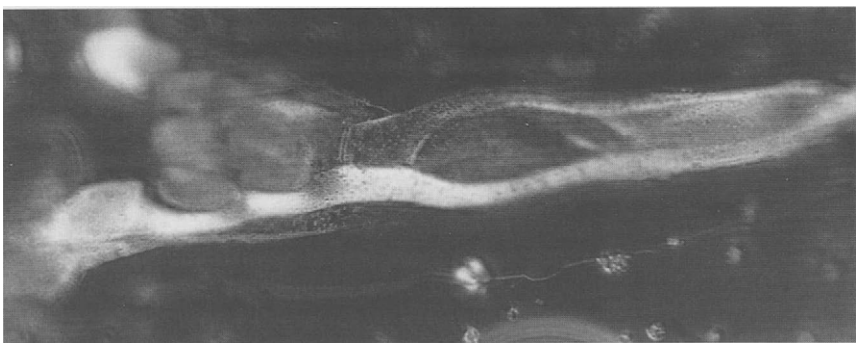

Figure XI.16: *Edge of a bond point in a light fabric, overbonded, fibers escaping to the perimeter. Cross section 1μm, differential interference contrast.*

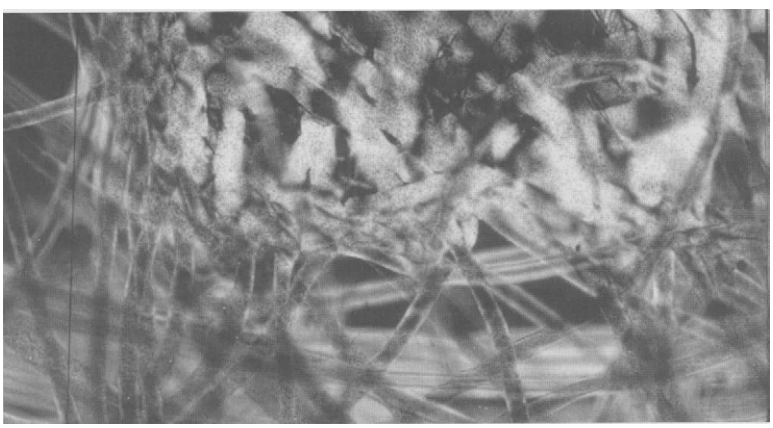

Figure XI.17: *Top view of a close to the optimum bond point quality, medium weight fabric. Differential interference contrast.*

short distances between them.

XI.3 Properties of Fabrics

The fabric properties depend on the properties of the individual fibers and on the strength of the fiber bonds. Morphology of the fibers is of a great significance. Theoretical calculations of the mechanical properties of nonwovens were conducted by Haerle and Newton,[18], Żurek[19] using analytical approaches, and Walczak[15] applying numerical methods to the discrete point bonded fabrics. In an effort not to cross over the boundaries of the subject matter of this book, only a summary of the spunbond properties are covered here.

The fabric morphology has the overpowering influence on the fabric strength, mainly the fiber directionality and strength of the individual fibers. The fiber directionality depends on the methods and equipment used to deposit the fibers

on the conveying wire. The fiber bending modulus has a very small, practically negligible influence. As for the fiber strength, the matters are not quite as straight forward. Thermal bonding, as any other heat treatment, does have an influence on the entire stress-strain curve of fibers.

The numerical calculations[15] permitted us to use the entire stress strain curve, rather than just a constant value of the modulus or any other simplification. It has been found that the stress-strain curve of fibers removed from bonded fabrics could be described by the general model as given in the equation XI.26[19].

$$\sigma = A\varepsilon + B[1 - \exp(-k\varepsilon)] \tag{XI.26}$$

Here σ is extensional stress, ε is extensional strain, A, B, and k are constants. The majority of stress-strain curves of the unbonded fibers could be described very successfully with the following formula.

$$\sigma = A\varepsilon^b \exp(-k\varepsilon) \tag{XI.27}$$

In the last equation A and b are constants.

The difference in the equations describing the stress-strain curves indicates the great depth of the changes suffered by the fibers as a result of heat exposure. This explains also why in the previous section so much emphasis was put on the protection from excessive heat exposure of those segments of fibers which do not form bond points.

Somewhat surprisingly, the initial modulus has a very strong influence on fabric strength. For example, an increase of the initial fiber modulus by a factor of 8.3 in an anisotropic fabric gives an insignificant increase of strength in the 0° (machine) - direction at break elongation smaller by about 25%. In the 90° (transverse) - direction, the strength is 15% higher and break elongation 15% lower.

The area occupied by the bond points has little influence on the fabric strength when more than some five per cent of the fabric surface is covered by bond points; strength increases slightly up to six or seven per cent of bond area. Below five per cent area, however, the decrease of fabric strength with the decreasing bond area is quite dramatic.

When the fiber morphology is highly anisotropic, bond point area has a somewhat larger effect on the tensile strength in the directions transverse to the machine direction. The pattern of bond point distribution, as well as the size of the individual points have very little influence on tensile properties.

Tear strength of nonwoven fabrics shows very similar dependencies as the tensile strength; bond point pattern and bond point area have even a little smaller influence on tear than on tensile strength.

Bending modulus is a very important property. It governs such subjective fabric properties as "drape" and "pliability", those properties in which nonwovens are by their nature deficient. But here we have a surprise: boding pattern has a very significant influence on bending modulus. The earlier attempts at calculation of bending[20,21] gave results showing large discrepancies with experimental data.

Żurek[22] suggested that the discrepancies may be the result of the fact that buckling of the fibers was not taken into account.

Microscopic investigations[15] of fabric bending show that, contrary to the normal treatment of bending bars or plates, the neutral plain is not located in the middle of the specimen thickness, but rather on the surface which bends over the largest radius. This results from the fact that the force needed to extend a fiber is many times greater than the force needed to buckle it. Even in case of nonwovens made of elastic polyurethanes, the neutral plane, depending on the type of polymer, is either on the surface with the largest radius or closely under this surface, never in the center.

If the above is taken into consideration, the results are easy to predict. Such morphologies show low bending modulus which have long fiber segments between bonds. The length facilitates buckling. Often the length of fibers between bond points in a fabric is uneven; in such cases, the larger the fraction of long segments, the lower the bending modulus. Also, space is needed for the fibers to buckle, so for lower bending force the fabric density ought to be low.

Naturally, where bending modulus of a nonwoven fabric is of particular importance, elastomeric fibers or crimped fibers would be the obvious choice of fibers. Unfortunately, so far no spunbond process resulting in crimped fibers is known.

Abrasion resistance belongs to the group of more important textile properties. In the case of nonwovens, the mechanism of abrasion is somewhat complicated. If the abrading force acts parallel to the fibers, then the fiber resistance is higher. If the force acts perpendicular to the fibers, their resistance depends on the fiber length between the bonds. When the force acts perpendicularly, then the fibers behave similarly to a sling, and in this case the fiber resistance depends primarily on its ability to recover from deformation.[22] In pure abrasion, such as that under forces acting parallel, the resistance of fibers is inversely proportional to their tenacity.

XI.4 Spunbonded from Solution

Dry fiber formation from solution has an important advantage. If the fibers are collected on the transporting wire with an impact, and if at the moment of impact the fibers are still tacky, incompletely dry, then the process is *self bonding*. This means that the bonding is accomplished in one operation with the fiber formation.

The self bonding process is advantageous not only from the point of view of economy: there may be little differentiation in the bond strength across the fabric thickness. With other bonding techniques providing for uniform bonding across the fabric thickness is difficult; a tendency to delamination is observed, and the tendency grows with the increasing fabric thickness.

Theoretically, wet formation may yield selfbonded spunbonded materials; the inherent slowness of the wet processes, however, collides with the commercial interests. There are known spunbond processes utilizing dry formation from solution, but they employ nonconventional formation methods: electrostatic[24] or centrifu-

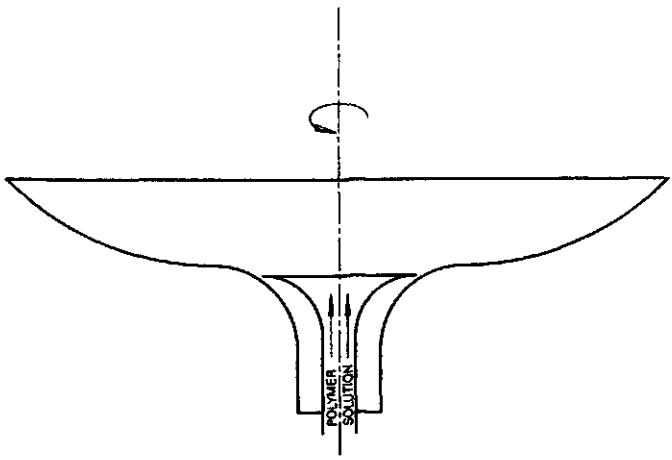

Figure XI.18: *Schematic sketch of the rotating cup used for centrifugal- electrostatic fiber formation. According to J. Fine and S. de Tora.*[25]

gal - electrostatic.[25] None of the processes has achieved great commercial success. However, the centrifugal-electrostatic process is capable of yielding very interesting products, and therefore it is given some attention here.

A filtered and metered polymer solution is introduced axially to a rotating cup, as in the schematic sketch in figure XI.18. Centrifugal force spreads the solution over the surface of the cup, with the increasing radius the solution layer becomes correspondingly thinner. In a properly running process, the viscosity of solution and velocity of rotation (the centrifugal force) must be so adjusted that the thin film of polymer solution splits into filaments on leaving the rim of the rotating cup. The splitting may actually take place on the rim itself or some five to six millimeters outward.

The centrifugal force throws the filaments out in a radial direction. To attract the fibers to the collecting wire an electriostatic field, of strength usually between some 50 and 120 KV,is applied between the rotating cup and the collecting wire. The distance between the cups and the collecting wire is so selected that the fibers adhere to each other on impact since they are not completely dry. The original patent suggests the spraying operation to be upwards, but with a little change in the design of the solution entry to the cup, the configuration may be reversed to a downward spraying.

Solvents of low electrical conductivity must be used to avoid discharges in the electric field. All the machinery must be in an enclosure which serves as a drying chamber, and this is one of the points which makes the process somewhat cumbersome.

To provide for high basis weight uniformity, the rotating bells are made to oscillate in the direction perpendicular to the wire motion. The natural pattern from one bell is a ring with fiber lay down density of approximately normal distribution in the radial direction.

The original process was capable of producing exceptionally uniform fabrics of a wide range of surface weights. Fibers of ten micron or less are easily obtainable. Polyurethane solutions gave very delicate fabrics of very interesting properties. If the individual fibers are around ten microns or less, then elastomeric fibers do not have any rubbery appearance, they are rather soft and velvety. Fine fibers of some elastomeric polymers other than polyurethanes may be obtained also in the meltblown process. Nevertheless, meltblown fabrics must be bonded and in this operation the exceptional properties of fabrics are lost. The electrostatic - centrifugal process is also well suited for laminations.

Many other polymers may be used in the process, however, the fibers cannot be cold drawn, so only such polymers which do not require drawing are really suitable.

XI.5 References

1. W. Żurek: *Struktura przędzy* (Structure of yarn), Wydawnictwa Naukowo - Techniczne, 2^{nd} Ed., Warszawa, 1971.
2. W. Żurek and A. Kopias: *Struktura płaskich wyrobó włókien-niczych* (Structure of flat textile products), Wydawnictwa Naukowo – Techniczne, 2^{nd} Ed., Warszawa, 1983.
3. *U. S. Pat.* **No. 3,352,734 (1967)**, to Imperial Chemical Industries.
4. *U. S. Pat.* **No. 3,341,394 (1967)**, to E. I. Du Pont De Nemours.
5. *U. S. Pat.* **No. 3,117,055 (1964)**, to E. I. Du Pont De Nemours.
6. *U. S. Pat.* **No. 3,368,934 (1968)**, to E. I. Du Pont De Nemours.
7. F. W. Manning, *U. S. Pat.* **2,411,660.**
8. V. A. Wente, *Tech. Report No. PB111437, Naval Research Lab.*, **NRL - 4364, 4/15/1954.**
9. R. L. Shambough, *Ind. Eng. Chem. Res.*, **27 (1988)**, 2363.
10. M. A. J. Uyttendaele and R. L. Shambough, *AIChE., J.*, **36 (1990)**, 175.
11. T. T. Wu and R. L. Shambough, *Ind. Eng. Chem. Res.*, **31 (1992)**, 379.
12. R. S. Rao and R. L. Shambough, *Ind. Eng. Chem. Res.*, **32 (1993)**, 3100.
13. H. Bodaghi, *INDA JNR*, **1, No.** 1, 14.
14. T. A. Zack, A. S. Curro, K. R. Randall: *New Developments in Through - Air Bonding*, paper presented at *Index 84* Congress, 1984.
15. A. A. Buykis and Ya. Ya. Tehts, *Primen. Modif. Polim. Mater. Konstr. Melior. Sist.*, **(1983)**, 54.
16. S. B. Warner, *Text. Res. J.*, **59 (1989)**, 151.
17. Z. K. Walczak: *Thermal Bonding of Fibers*, Kimberly - Clark Corp., Dalla – Atlanta – Neenah, 1992.
18. C. L. Choy, *Polymer*, **18 (1977)**, 984.
19. D. Hands, K. Lane, and R. P. Sheldon, *J. Polymer Sci., Symposia*, **No. 42 (1973)**, 717.
20. J. W. S. Haerle and A. Newton, *Text. Res. J.*, **37 (1967)**, 778.

21. it ref. 2, pp. 294 ff.
22. W. D. Freeston, Jr. and M. M. Platt, *Text. Res. J.*, **35 (1965)**, 48.
23. S. M. Lee and S. Argon, *Text. Res. J.*, **74 (1983)**, 1; 12.
24. *ref. 15*, p. 226.
25. *ref. 15*, p. 253.
26. *Ca. Pat.* **No. 937,827 (1973)**, to Farbenfabriken Bayer 26
27. J. Fine and S. A. De Tora, *U. S. Pat.*, **No. 4,223,101 (1980)**, to Inmont Corp.